



## Shallow water table effects on water, sediment and pesticide transport in vegetative filter strips: Part B. model coupling, application, factor importance and uncertainty

Claire Lauvernet<sup>1</sup> and Rafael Muñoz-Carpena<sup>2</sup>

5 <sup>1</sup>Irstea, UR MALY, centre de Lyon-Villeurbanne, 5 rue de la Doua-CS 70077, F-69626 Villeurbanne cedex, France.

<sup>2</sup>University of Florida, Agricultural and Biological Engineering, 287 Frazier Rogers Hall, PO Box 110570 Gainesville, FL 32611-0570, USA

*Correspondence to:* Claire Lauvernet ([claire.lauvernet@irstea.fr](mailto:claire.lauvernet@irstea.fr))

**Abstract.** Vegetative filter strips are often used for protecting surface waters from pollution transferred by surface runoff in agricultural watersheds. In Europe, they are often prescribed along the stream banks, where a seasonal shallow water table (WT) could decrease the buffer zone efficiency. In spite of this potentially important effect, there are no systematic experimental or theoretical studies on the effect of this soil boundary condition on the VFS efficiency. In the companion paper, we developed a physically-based numerical algorithm (SWINGO) that allows representing soil infiltration with a shallow water table. Here we present the dynamic coupling of SWINGO with VFSSMOD, an overland flow and transport mathematical model to study the WT influence on VFS efficiency in terms of reductions of overland flow, sediment and pesticide transport. This new version of VFSSMOD was evaluated with two contrasted benchmark field studies in France (sandy-loam soil under Mediterranean semi-continental climate, and silty-clay under temperate Oceanic climate), where testing of the model with field data showed promising results. The analysis showed that for the conditions of the studies, VFS efficiency decreases markedly when the water table is 0 to 1.5 m from the surface. In order to evaluate the relative importance of WT among other input factors controlling VFS efficiency, two global sensitivity and uncertainty analysis (GSA) methods, Morris and eFAST, were applied on the benchmark studies. The most important factors found for VFS overland flow reduction were saturated hydraulic conductivity and WT, added to sediment characteristics and VFS dimensions for sediment and pesticide reductions. The relative importance of WT varied as a function of soil type (most important at the silty-clay soil) and hydraulic loading (rainfall + incoming runoff) at each site. The presence of WT introduced more complex responses dominated by strong interactions in the modelled system response, reducing the predominance of saturated hydraulic conductivity on infiltration under typical deep water table conditions. This study demonstrates that when present, WT should be considered as a key hydrologic factor in buffer design and evaluation as a water quality mitigation practice.

10

15

20

25



## 1 Introduction

30 Today, surface waters are threatened by pesticide pollution at the local, regional and global scales (Malaj et al., 2014; Stehle and Schulz, 2015). Agricultural surface runoff is an important contributor to this contamination (Louchart et al., 2001). Grass buffer zones or vegetative filter strips (VFS), are a typical environmental control practice to protect aquatic ecosystems from sediment, and agrichemicals from agricultural fields (Roberts et al., 2012). While VFS are recommended in the USA and other regions, in Europe they are often mandatory along rivers due to their potential to limit surface pesticide runoff and aerial spray drift from entering adjacent surface water bodies (Asmussen et al., 1977; Rohde et al 1980; USDA-NRCS, 2000; 35 Dosskey, 2001; Syversen and Bechmann, 2004; Poletika et al., 2009). However, the effectiveness of edge-of-field buffer strips to reduce runoff transport of pesticides can be very different as a function of many local characteristics (land use, soil, climate, vegetation and pollutant). For example, based on 16 field studies (Reichenberger et al., 2007), the 25th percentile of VFS pesticide reduction efficiency ranges from 45 to 75 % of the amount coming into the filter from the field edge.

40 Moreover, VFS are typically located down the hillslope along the hydrographic network. As a result, the filter is often bounded by a seasonal shallow or perched water table, which may significantly inhibit their function and must be taken into account when designing VFS and evaluating their efficiency (Lacas et al., 2005). Dosskey et al. (2001, 2006) identified presence of shallow water table (<1.8 m) as an important factor that should be considered for VFS design and evaluation. Simpkins et al. (2002) also report that the hydrogeologic setting, specifically the direction of groundwater flow and the 45 position of the water table in thin sand aquifers underlying the buffers, is probably the most important factor in determining buffer efficiency. Arora et al. (2010), in a review on VFS pesticide retention from agricultural runoff present that soil saturation from a shallow water table may be a reason for negative runoff volume retention. Other studies also identify the potential effects of location of the buffers where shallow water table is present (Ohliger and Schulz, 2010; Borin et al., 2004) but do not quantify or study its effects (Lacas et al., 2005).

50 The processes occurring in the VFS interact in a complex manner in space and time, thus they must be simulated by dynamic models accounting for hydrologic (Gatel et al., 2016) and sedimentological variability (Fox et al., 2005). The Vegetative Filter Strip Modeling System (VFSSMOD) (Muñoz-Carpena et al., 1993, 1999; Muñoz-Carpena and Parsons, 2004) is a storm-based numerical model coupling overland flow, water infiltration and sediment trapping in a filter considering incoming surface flow and sediment from an upslope field (Fig. 1). VFSSMOD also includes a generalized empirical pesticide 55 trapping equation as a function of soil and sediment sorption, dissolved phase infiltration, and sorbed phase sedimentation (Sabbagh et al., 2009). Pesticide degradation on the filter is included between runoff events for long-term pesticide assessments (Muñoz-Carpena et al., 2015), but neglected during events due to their short duration (min to h). VFSSMOD has been successfully tested against measured data for predictions of flow, infiltration, and sediment trapping efficiency (Muñoz-Carpena et al., 1999, Abu-Zreig, 2001, Dosskey et al., 2002, Fox et al., 2005, Han et al., 2005, Pan et al., 2017), tracers and 60 multi-reactive reactive solutes (Perez-Ovilla, 2010), phosphorus (Kuo and Muñoz-Carpena, 2009), pesticides (Poletika et al., 2009; Sabbagh et al, 2009; Winchell et el., 2011), and colloids (Yu et al., 2013). Previous work studied the global sensitivity



of simulated outflow, sediment and pesticide trapping to VFSSMOD input factors (Muñoz-Carpena et al., 2007, 2010, 2015; Fox et al. 2010). At the watershed scale, VFSSMOD has been included in methods or frameworks to optimize filter placement and design (Dosskey et al., 2006; Tomer et al., 2009; White and Arnold, 2009; Balderacchi et. al, 2016; Carluer et al., 2017).  
 65 Sabbagh et al. (2010) integrated VFSSMOD within higher-tier, US-EPA long-term pesticide exposure framework (PRZM/VFSSMOD/EXAMS) to estimate changes in aquatic concentrations when VFS are adopted as a runoff pollution control practice.

The extended Green-Ampt soil infiltration component used in VFSSMOD does not account for the presence of a shallow water table (Skaggs and Khaheel, 1982). In a companion paper, a physically-based algorithm was developed to describe soil  
 70 infiltration under shallow water table conditions (SWINGO: Shallow Water table Infiltration alGOrithm). Dynamic coupling of this new infiltration algorithm to VFSSMOD will allow for mechanistic description of interactions between surface and subsurface hydrology under shallow water table boundary conditions and ensuing effects on VFS sediment and pesticide transport.

Thus, the objective of this work is to study the effects that the change in infiltration introduced by the presence of shallow  
 75 water table has on VFS runoff reduction, sediment and pesticide trapping. This was done by a) dynamic coupling of SWINGO in VFSSMOD; b) evaluating the coupled model on two contrasted benchmark study sites (sandy-loam soil vs silty-clay soil) and events (Mediterranean semi-continental vs temperate oceanic climates); and c) global sensitivity and uncertainty analysis to ascertain the actual global importance of shallow water table depth on the efficiency of the VFS when compared to other input factors.

## 80 2 Material and methods

### 2.1 Dynamic coupling of shallow water table infiltration algorithm (SWINGO) with VFSSMOD overland flow, sediment and pesticide components

The overland flow submodel in VFSSMOD (Muñoz-Carpena et al., 1993a) (Fig. 1) is based on the kinematic wave equation numerical, upwinding Petrov-Galerking finite element (FE) solution (Lighthill and Whitham, 1955),

$$85 \begin{cases} \frac{\partial h}{\partial t} + \frac{\partial q}{\partial x} = i - f = i_e \\ S_f \approx S_o \rightarrow q = \frac{\sqrt{S_o}}{n} h^{5/3} \end{cases} \quad (1)$$

with initial and boundary conditions

$$\begin{cases} h = 0; 0 \leq x \leq VL, t = 0 \\ h = h_o; x = 0, t \geq 0 \end{cases} \quad (2)$$

where  $h=h(x,t)$  [L] is the flow depth,  $t$  is time (L),  $q=q(x,t)$  [L<sup>2</sup>T<sup>-1</sup>] is discharge per unit width,  $x$  [L] is the surface flow direction axis,  $i=i(t)$  [LT<sup>-1</sup>] is rainfall intensity,  $f=f(t)$  [LT<sup>-1</sup>] is soil infiltration rate,  $i_e=i_e(t)$  [LT<sup>-1</sup>] is rainfall excess,  $S_o$  and  $S_f$   
 90 [LL<sup>-1</sup>] are the bed and water surface friction slopes at each node of the system,  $n$  is Manning's surface roughness coefficient,



$VL$  [L] is the filter length, and  $h_o=h_o(0,t)$  [L] represents the field runoff hydrograph entering the filter as a boundary condition (Fig. 2).

Originally, the overland flow component was coupled for each time step with a modified Green-Ampt infiltration algorithm for unsteady rainfall (GAMPT, see Fig. 1) for soils without (or with deep) water table (Chu, 1978; Mein and Larson, 1971, 1973; Skaggs and Khaheel, 1982; Muñoz-Carpena et al., 1993b). The infiltration component provides the rainfall excess,  $i_e$  in Eq. (1), based on a given rainfall distribution (hyetograph) for each FE node and time step. The field conditions can be well represented since the program handles field inflow hydrographs and hyetographs, and spatial variability of the filter over the nodes of the grid (Fig. 2).

In the sediment component (Fig. 1), based on sediment mechanics (transport and deposition) in shallow flow, the model divides the incoming sediment into bed load (coarse particles, with diameter  $>37 \mu\text{m}$ ) and suspended load (fine particles, diameter  $<37 \mu\text{m}$ ). Bed load deposition is dynamically calculated based on Einstein bed-load transport equation successfully tested for variable shallow flow through non-submerged dense vegetation (Barfield et al., 1978). Transport and deposition of suspended particles is calculated for non-submerged dense vegetation conditions (Tollner et al., 1976; Wilson et al., 1981). Flow characteristics needed for sediment calculations are provided for each time step by the overland flow component. The particle deposition pattern on the filter is predicted based on a conceptual sediment wedge, mass-balance approach (Fig. 2a). Pesticide reduction and transport in the filter during the runoff event is calculated within the water quality/pollutant module (Fig. 1) based on a generalized regression-based approach developed from on a large database of field studies by Sabbagh et al. (2009) and further tested by others (Poletika et al., 2009; Winchell et al., 2011). The equation considers reduction of dissolved pesticide through infiltration, deposition of sediment-bound pesticide, and pesticide adsorption characteristics. The integration of the mechanistic (flow and sedimentation from VFSMOD) and empirical pesticide approaches allows for identification of important site-specific factors determining the efficiency of pesticide removal (or lack of thereof) under realistic field conditions (Muñoz-Carpena et al., 2010; Fox et al., 2010).

In this work, to simulate VFS water, sediment and pesticide dynamics under realistic unsteady rainfall-runoff conditions for shallow water table conditions, we dynamically couple the new algorithm SWINGO (developed in the companion paper) as an alternative, user-selected infiltration submodel (Fig. 1). Full details of SWINGO are provided in the companion paper. Briefly, SWINGO is a time-explicit infiltration solution based on a combination of approaches by Salvucci and Entekhabi (1995) and Chu (1997) with the assumption of a horizontal wetting front. Proposed integral formulae allow estimation of the singular times: time of ponding ( $t_p$ ), shift time ( $t_o$ ), and time ( $t_w$ ) when the wetting front depth is equal to  $z_w$  (capillary fringe above the water table, Fig. 2b). As with GAMPT described above, the algorithm provides the infiltration rate  $f$  (Eq. 1) for each FE node and time step  $t_j$  as,

$$\begin{cases} f = i & 0 < t < t_p \\ f = f_p = K_s + \frac{1}{z} \int_0^{L-z} K(\psi) d\psi & t_p < t < t_w \\ f = \min(f_w, i) & t \geq t_w \end{cases} \quad (3)$$



where (Fig. 2b),  $z$  [L] is the vertical axis,  $L$  [L] the depth to the water table,  $K=K(\psi)$  [ $\text{MT}^{-1}$ ] the soil water hydraulic conductivity function of soil matric potential  $\psi$  [L] (non uniform with depth),  $K_s$  [ $\text{MT}^{-1}$ ] is the saturation soil water content, and  $f_w$  [ $\text{MT}^{-1}$ ] is the end vertical boundary condition when the wetting front reaches the water table (or its capillary fringe) typically assumed as vertical saturated flow or lateral drainage (see companion paper for details). For real VFS field situations, unsteady rainfall without initial ponding must be considered and  $t_p$  and  $t_o$  calculated. For each time step increment,  $\Delta t=t_j-t_{j-1}$ , the surface water balance at each VFS FE node (neglecting evaporation during the event) (Chu, 1997) is,

$$\Delta P = \Delta F + \Delta S + \Delta RO \quad (4)$$

where  $\Delta P$ ,  $\Delta F$ ,  $\Delta S$ , and  $\Delta RO$  [L] are changes for each  $\Delta t$  of cumulative precipitation ( $P$ ), cumulative infiltration ( $F$ ), surface storage and cumulative excess rainfall ( $RO$ ). Notice that  $i_e = \Delta RO / \Delta t$  for each time step. Unsteady rainfall is described by a hyetograph of constant  $i_j$  for each rainfall period. If surface storage becomes  $s=0$  then  $t_p$  and  $t_o$  are re-calculated at the next rainfall period as,

$$t_p = \frac{1}{i_j} \left[ \left( \theta_s z_p + \int_L^{L-z_p} \theta(h) dh \right) - P(t_j) + RO(t_j) \right] + t_j \quad (5)$$

$$t_o = \int_0^{z_p} \left[ \frac{\theta_s - \theta(L-z)}{f(z)} \right] dz \quad (6)$$

where  $\theta_s$ ,  $\theta(h)$  [ $\text{L}^3 \text{L}^{-3}$ ] are the soil water saturated content and the soil water characteristic curve, and  $z_p$  [L] is the equivalent wetting front depth at  $t_p$ , and for periods after the first  $z_f(t)=z_p(t)$  (Fig. 2b) is calculated explicitly from the Newton-Raphson iterative solution ( $k$  iteration level),

$$z_p^{k+1} = z_p^k - \frac{G(z_p^k, t)}{\frac{dG(z_p^k, t)}{dz}} \quad \text{with} \quad |z_p^{k+1} - z_p^k| < \epsilon \quad \left| \begin{array}{l} G(z_p^k, t) = t - t_p - t_o - \int_0^{z_p} \frac{\theta_s - \theta(L-z)}{K_s + \frac{1}{z} \int_0^{L-z} K(\psi) d\psi} dz \\ \frac{dG(z_p^k, t)}{dz} = - \frac{\theta_s - \theta(L-z)}{K_s + \frac{1}{z} \int_0^{L-z} K(\psi) d\psi} \end{array} \right. \quad (7)$$

Finally, the algorithm computes  $t_w$ , the time to reach column saturation as,

$$t_w = t_p - t_o + \int_0^{z_w} \frac{\theta_s - \theta(L-z)}{f(z)} dz \quad (8)$$

Similarly, this singular time  $t_w$  has to be obtained again each time  $t_p$  and  $t_o$  are computed. When initial ponding is present we get  $t_p = t_o = 0$ . Additional details are provided in companion Paper 1, and Supp. Materials **S1** provides instructions for downloading the free VFSMOD open source code, documentation and sample applications.

## 2.2 Benchmark field studies

VFSMOD extended for shallow water table was tested and analyzed on two experimental VFS sites in France (Fig. 3, Table 1), selected because they represent contrasting agronomic, pedological and climatic conditions (Fontaine 2010). The first site



in a Beaujolais vineyard (Rhône-Alpes) consists of a vegetative filter strip on a steep hillslope (20-30%) located along the river Morcille (affluent of the Saône river). The site was instrumented from 2001 to 2008 for long-term experiments of infiltration-percolation of phytosanitary products (Boivin et al., 2007; Lacas, 2005; Lacas et al., 2012). The region has a semi-continental climate, with Mediterranean influence, where intense seasonal runoff events can induce erosion. The soil is a very permeable granitic sandy-clay. The water table is deep in summer and shallow in winter after intense storm events, from 60 cm deep at the downstream part of the strip near the river to 1.5 m deep at the field upstream side of the strip (Lacas, 2005).

The site of Jaillièrè (Loire-Atlantique, close to Brittany) is an experimental farm maintained by ARVALIS–Institut du Végétal where soils are shallow and hydromorphic, and climate is temperate oceanic with mild and rainy winters and cool and wet summers (Madrigal-Monarrez, 2004). Buffer zone experiments were conducted at the site under natural rainfall (Patty et al., 1997) and simulated runoff (Souiller et al., 2002). Crops are mainly wheat and maize, typically under tile drainage conditions, with slopes of around 3%. Silty clay soils overlay a virtually impermeable layer of alterite shales, typically leading in winter to the formation of seasonal shallow water table from 0.5 m to 2 m and the appearance of runoff by subsaturation (Adamiade, 2004).

Among the pesticides used at the experimental sites, a soluble and low sorption (mobile) herbicide (Isoproturon) used on both sites was selected for simulations, contrasted by a less mobile product chosen at each site, i.e. the fungicide Tebuconazole on Morcille and the herbicide Diflufenican on Jaillièrè (Madrigal et al 2002) (Table 1).

For each site, a set of around 20 of observed field events with shallow water table conditions was analyzed. These consisted of precipitation, field runoff and water table observations at both sites. Detailed hydrograph outflow from the VFS was also available for Morcille. One event considered as representative (i.e. significant enough to lead to surface runoff at the outlet of the VFS, but not extreme) was chosen for each site (Fig. 4a and 4b).

### 2.3 Global sensitivity analysis

Global sensitivity (GSA) and uncertainty analysis (UA) of the coupled model allows for the systematic study of the influence of the input factors and their interactions on VFS performance for surface runoff, sediment and pesticide removal. The “global” term denotes that GSA studies output variability when all input factors vary globally, within their validity domain defined by probability distribution functions (PDF), as opposed to locally, (one at a time), *i.e.* around an arbitrary range from a base value. GSA allows for simultaneous estimation of the factors individual importance and interactions (Saltelli et al., 2004). In this study, two complementary sensitivity methods were used: the qualitative Morris’ (1991) elementary effects screening method, and the quantitative variance-decomposition extended Fourier Amplitude Sensitivity Test (eFAST) (Cukier et al., 1978; Saltelli et al., 1999). In both methods, input factors are sampled, the model is evaluated on the sample sets, and global sensitivity indices are computed. Morris is generally used as a first, qualitative step to identify a group of important input factors, where in a second step a variance-based method is computed on the selected input factors (Saltelli et



al., 2007, 2008). In this study, both methods were run with the full set of inputs as a check for the consistency of the GSA  
180 results.

Morris method uses in its original form a regular discretization of the  $k$  input factors space defined by their PDFs, requiring a  
total number of simulations ( $N$ ) on the order of  $N=r(k+1)$  where  $r > 8$  is the number of sampling trajectories, typically taken  
as 10 (Campolongo et al., 2007). Each factor influence, called Elementary Effects (EE), is evaluated by comparison of  
simulations where this factor is changed alternatively among the others. Morris is a robust, low-cost sensitivity analysis that  
185 allows identifying quickly the most influent input factors without prior model assumptions (i.e. linearity, additivity)  
(Campolongo et al., 2007; Faivre et al., 2013; Khare et al., 2015). Sensitivity indices for each factor  $X_i$  ( $i=1, k$ ) are computed  
based on the EE: (i)  $\mu_i^*$  (mean of absolute values of EE) that measures *direct effects* of each factor on the output of interest,  
and (ii)  $\sigma_i$  (standard deviation of EE) that provides a measure of *interactions and non-linearities*. The method compares the  
input factors' indices relatively to the others, making possible to visually classify the inputs on a  $(\mu^*, \sigma)$  Cartesian plane in 3  
190 groups as a function of their relative effect on the model: (1) negligible effect (low  $\mu^*$  and low  $\sigma$ ), (2) important direct  
effects and small interactions (high  $\mu^*$  and low  $\sigma$ ), (3) important non-linear and/or interactions (high  $\mu^*$  and high  $\sigma$ ).

The eFAST method is a quantitative global sensitivity method based on high-dimensional variance decomposition. A  
pseudo-random multivariate sampling scheme is conducted across the  $k$ -dimensional space, informed by the input factors  
PDFs, requiring  $N=M*k$  simulations with  $M$  between 512 and 1024. The model total output  $Y$  variance is decomposed in  
195 parts attributed to each factor direct effects or to factor interactions. First order sensitivity indices ( $S_i$ ) for each factor  $X_i$  are  
defined by the fraction of the output variance associated to the direct effect of that factor and represents the average output  
variance reduction that can be achieved when the input factor  $X_i$  is fixed (Tarantola et al., 2002; Yang, 2011). Total  
sensitivity indices ( $S_{Ti}$ ) are calculated as the fraction of variance associated with that factor and its interactions. The largest  
values of the sensitivity indices correspond to the highest influence of these inputs on the corresponding output variable  
200 (Saltelli et al., 2008; Faivre et al., 2013). Since global sensitivity indices are computed from a dense randomized multivariate  
sampling, it is possible to exploit this sampling to perform uncertainty analysis by studying the probability distribution  
functions for each output of interest (Muñoz-Carpena et al., 2007). eFAST was chosen on this study because it is robust and  
overcomes the initial limitation of the Fourier Amplitude Sensitivity Test (Cukier et al., 1978) applicable only for mostly  
additive models (i.e.  $S_i > 0.6$ ) (Faivre et al., 2013). Interestingly, the Morris indices ( $\mu^*, \sigma$ ) have been found to provide a  
205 good approximation to the eFAST indices ( $S_{Ti}, S_{Ti}-S_i$ ) at a much lower computational cost (Saltelli et al. 2004, Campolongo  
et al. 2007) making it ideal for large and computationally expensive models.

## 2.4 Selection of inputs and outputs for GSA simulations

The first step of GSA is to define output variables and input factors. In this study, changes in VFS efficiency were selected  
as output variables: reduction of water (dQ), sediments (dE) and pesticides (dP). Both model versions, with water table  
210 (SWINGO algorithm) and without water table (GAMPT algorithm), were compared on each site. The input factors (Table 2)



were selected considering previous GSA performed on VFSMOD (Fox et al., 2010; Muñoz-Carpena et al., 2007, 2010), with new inputs for the water table case (OR, VGALPHA and VGN, L). Input factors distributions (Table 2) are assigned based either on experimental measurements on the case study plots, expert knowledge, or scientific publications.

Although the VFS dimensions FWIDTH and VL were measured on the field (Table 1), the effective dimensions are known to be different in practice as the runoff does not follow perfectly uniform sheet flow (Abu-Zreig, 2001). Thus, the measured values were chosen to vary uniformly within -10% and +10% for FWIDTH and VL, respectively (Muñoz-Carpena et al., 2010). The slope (SOA) uniform distribution represents field measured spatial variation across the VFS. PDFs for filter roughness and vegetation factors were assigned based on vegetation type (Table 1) (Haan et al. 1994; Muñoz-Carpena et al. 2007).

For the infiltration components, log-normal PDFs were assigned to the soil saturated hydraulic conductivity (VKS) from measured values at each site (Madrigal-Monarrez, 2004; Souiller et al., 2002; Lacas, 2005) based on effective field values calculated from the harmonic mean of the topsoil horizons (Bouwer, 1969). The Green-Ampt infiltration OI and OS inputs were fitted distributions based on values measured at the sites, and the average suction at the wetting front (SAV) was considered to vary uniformly based on ranges for soil texture at each site (Rawls et al., 1983). Soil water characteristics parameters (VGALPHA, VGN, OR) needed for calculation of infiltration under shallow water table (Eq. 3-8) were assigned normal PDF based on the soil texture (Meyer et al., 1997). Hourly water table depths (L) that were automatically monitored on Morcille during the case study event (Lacas, 2005) followed a uniform distribution. On Jaillièrè, the average water depth and variation was measured manually at the site (Adamiade, 2004) and a uniform distribution around these values assigned.

Sediment particle characteristics from the upper field (COARSE and DP) were assigned uniform distributions based on USDA textural class (Woolhiser et al., 1990), and truncated to respect the relationship between DP and COARSE (Muñoz-Carpena et al., 1999).

For pesticide inputs, field measurements of the percentage of clay (PTC) and organic carbon (PCTOC) of the upper field followed a uniform PDF (Lacas, 2005; Benoit et al., 1998; Madrigal-Monarrez, 2004). The triangular distribution for KOC for the pesticides evaluated at each site is based on measurements; in Jaillièrè for the base value and boundaries (Benoit et al., 1998; Souiller et al., 2002), and in Morcille for the base value (Lacas, 2005) but using boundaries from PPDB database (UIPAC, 2007).

In all, considering the two sites, two infiltration options (GAMPT without shallow water table with  $k=18$ , and SWINGO with shallow water table with  $k=20$ , Table 2) and 2 pesticides at each site, the total number of GSA simulations performed were 75544 for eFAST ( $M=497\approx 500$ ) and 1600 for Morris. The procedure was repeated 3 times to ensure the robustness of the results.

### 3. Results



### 3.1 Model application on benchmark studies

The effect of water table on simulated VFS efficiency using SWINGO was first tested on the two contrasted benchmark study sites Morcille (Fig. 4a) and Jaillièrre (Fig. 4b). Since a stream at the bottom of the VFS was present on both sites, the lateral Dupuit-Forscheimer option was selected for the end vertical boundary condition  $f_w$  (Eq. 3) (see section 2.1 in companion paper). The detailed outflow hydrograph from the VFS measured during the event at Morcille is compared with a direct simulation with base values (no calibration) (Fig. 4a). The dashed line for  $L=2.5$  m corresponds to average measured VKS for the top soil horizons ( $4.58E-05$  m/s), and the grey envelope represents outflow variability due to uncertainty of measured hydraulic conductivity (between  $3.89E-05$  m/s from direct measurement on the soil surface horizon 10-30 cm and  $5.29E-05$  m/s computed by harmonic mean of measurements on 0-10 cm and 10-30 cm horizons). In addition to the measured water table depth at the sites, each event was tested with different water table conditions to study the response to these conditions (Fig. 4a,b). The large differences in VFS surface outflow found between shallow and deeper water table clearly illustrates the hydrological importance of shallow water table presence on VFS at these sites.

Direct simulation of the VFS surface outflow at Morcille fits observations well for the end of the second rain period (4000 to 6000s) but misses the rest (Fig. 4a). The differences between simulated and observed values could come from measurement errors at the site, since runoff was expected early on for an event with such hydraulic loading (rainfall + incoming runoff). The intrinsic spatial variability of  $K_s$  represents also a significant source of uncertainty (grey area in Fig. 4a). In all, considering that base values without calibration were used in the simulation, the results are deemed satisfactory.

The effect of water table change (from 0-2 m) on VFS changes in runoff (dQ), sediment (dE) and pesticide (dP) reductions for the two case studies is presented in Fig. 5. In general, dQ and dP are sensitive to the shallow water table depth until a threshold ( $\sim 1.5$  m for the case study sites) beyond which there are no effects and the filter achieves maximum efficiency for the event. The two-step curves for Morcille are due to the two storm periods, where relative contributions to surface flow between the first and second events will vary with the depth of the shallow water table. Sediment retention (dE) does not exhibit similar changes because the relatively low flow conditions experienced likely result in low transport capacity available and high sediment deposition on the VFS. The difference in effects introduced by the chemical characteristics of the pesticide is observed in the curves for Diflufenican (high sorption) and Isoproturon (low sorption) at Jaillièrre. This local study does not take into account all effects and interactions between input factors, but only the water table depth variation effect. A global sensitivity analysis presented in section 3.2 will address this.

The simulation results for Morcille and Jaillièrre confirm that a shallow water table can affect the VFS surface hydrological response by generating saturation surface runoff, depending on the soil characteristics and the hydraulic loading. Conversely, for deep water table, surface hydrology processes are effectively decoupled after a threshold controlled by the soil characteristics and hydraulic loading. Interestingly, simulations with the no shallow-water table option (GAMPT, Fig. 1) for the case study conditions closely matched those for SWINGO for the deeper water tables in Fig. 4, providing additional physical consistency to both components.



### 275 3.2 Global sensitivity analysis of water, sediment and pesticide reductions

A combination of shallow water table (“WT”, run with SWINGO) and no shallow water table (“no WT”, run with GAMPT) simulations (Fig. 1) for Jaillière and Morcille conditions with two pesticides at each site (Table 1) were selected for GSA Morris and eFAST methods. For simplicity, GSA results from Morris and eFAST are presented only for one pesticide, Isoproturon, which is a common herbicide with average soluble properties. A comparison of the different pesticides effects is presented in the uncertainty analysis section later.

#### Qualitative analysis: method of Morris

Morris sensitivity analysis indices (Table S1 in Supp. Materials) are presented in Fig. 6, where important input factors for each output are separated from the origin of the ( $\mu^*$ ,  $\sigma$ ) Cartesian planes. Distinct patterns on the important factors controlling the shallow water table effects on the efficiency of the VFS (dQ, dE, dP) are identified by comparing the different soil (fine at Jaillière and coarse at Morcille) and hydraulic loading across the study sites. The differences can be interpreted in terms of the interplay between excess rainfall (controlled mainly by the saturated hydraulic conductivity VKS and hydraulic loading) and sub-saturation (controlled by the water table depth L).

Finer soils typically exhibit lower permeability but a higher capillarity fringe above a water table (Terzaghi, 1943; Lane and Washburn, 1946; Parlange et al., 1990). For no WT, excess rainfall (controlled by VKS) leads to relatively more water on the surface compared to coarse soils. Morris results (Fig. 6a) show the strong sensitivity of dQ to VKS for this case. With WT the soil readily sub-saturates and it is less sensitive to VKS. This is shown by the strong direct effect of L on dQ (Fig. 6d). For dE in finer soils, more runoff present at the surface typically results in higher transport capacity available, and sediment and surface characteristics become a limiting factor for transport and deposition (Muñoz-Carpena et al., 2010). This is shown by the importance of DP and interaction with VKS (Fig. 6b). This is exacerbated with WT, where excess rainfall no longer controls surface flow and VKS falls in importance while sediment and surface characteristics dominate the response (Fig. 6e). In general, pesticide reduction (dP) is controlled by factors controlling the liquid (dQ) and solid (dE) phase transport (Sabbagh, et al., 2009). For no WT and for this moderately adsorbed chemical, the effect of excess rainfall on dQ (controlled by VKS) also becomes the most important process for dP (Fig. 6c). With WT, the dominance of L in dQ is also present in dP, with some sediment and pesticide characteristics also showing importance (Fig. 6f).

In contrast, the coarser soil in Morcille exhibits higher permeability and small capillary fringe and under no WT runoff is typically controlled by excess rainfall (importance of VKS on Fig. 6g). With WT, the soil might sub-saturate depending on position L and this input gains importance interacting with VKS (Fig. 6j). For dE and no WT (Fig. 6h), with more permeability the surface water flow (controlled by VKS) is the main limiting factor controlling sedimentation (Muñoz-Carpena et al., 2010). With WT, again the VKS and L that control surface flow also interact strongly to control sedimentation, and sediment soil water characteristics are of secondary importance (Fig. 6k). Control of infiltration



propagates also into dP, and for this moderately sorbed pesticide, dQ factors also control dP (Fig. 6i,l).

Interestingly, introduction of WT increases the number of factors and interactions (i.e. more input factors show higher  $\sigma$  values and are separated near or above the dashed 1:1 line). This indicates an increase in complexity of the VFS response when the shallow water table is present. This suggests that simple relationships to simulate water, sediment and pesticide behavior are not able to represent all complex processes that interact in a VFS.

### Quantitative analysis: eFAST method

Figure 7 further quantifies the input factor effects in terms of changes to the output variance (see also Table S2 in Supp. Materials). Comparison of eFAST (Fig. 7) and Morris (Fig. 6) indices for interactions and first order effects,  $S_{Ti}-S_i \sim \sigma$  and  $S_{Ti} \sim \mu^*$ , respectively, shows good consistency among the methods (Saltelli et al, 2004; Campolongo et al, 2007) and further corroborates the results.

The importance of VKS for both soils under no WT identified by Morris is quantified by more than 90% of the dQ and dP output variance being controlled by first order (direct) effects of this factor (Fig. 7a,g and 7c,i). Similarly, the importance of DP for dE for the fine soil is apparent where more than 60% of the variance is explained by this first order and interaction effects of this factor (Fig. 7b,e). For the case of WT, the effect of L on dQ and dP is predominant, with 60-90% of the output controlled by this factor and its interactions (Fig. 7).

The sum of first order indices quantifies the model additivity for each output variable ( $\sum S_i$  insets in Fig. 7), and the visible exceeding black area in the bars, i.e. difference between total and first order ( $S_{Ti}-S_i$ ) for each input factor, represents factor interactions. In general, the decrease in  $\sum S_i$  values and increased black bar areas (Fig. 7d-f and j-l) support the Morris finding of increased complexity of the system responses in presence of a shallow water table.

### Uncertainty Analysis

The dense multivariate sampling used in eFAST allows realizing a formal uncertainty analysis of water (dQ), sediment (dE), pesticide (dP) reduction outputs for the 2 contrasted pesticides at each site (Fig. 8 and Table S3 in Supp. Materials). As expected, the reduction in infiltration and increase in surface flow introduced by the shallow water table translates into a distinct decrease in dQ values, with median dQ changing from 81% to 7% and 65% to 45% in Jaillièrè (Fig. 8a, b) and Morcille (Fig. 8c,d), respectively (Table S3, Supp. Materials). For dE, for the coarser soil at Morcille the smaller change in dQ with WT does not visibly change the high sediment retention, whereas for the finer soil of Jaillièrè the changes in flow introduce marked changes in median dE from 99% to 64%. Again, changes in dQ and dE with WT affect the VFS pesticide retention at both sites, with median reductions from dP = 99% to 38% and 97% to 84% in Jaillièrè and Morcille, respectively. Since the VFS pesticide retention is also directly related to pesticide sorption characteristics (Sabbagh et al., 2009), some differences are expected for different chemicals. Reduction of Diflufenicanil on Jaillièrè (dP-Dif) (Fig. 8b) and Tebuconazole on Morcille (dP-Teb) (Fig. 8d) is higher than the other two pesticides because of their affinity for sediment



(higher KOC values in Table 1) and high sediment retention in the VFS.

340 These results further support the GSA findings that changes in surface and subsurface hydrological responses introduced by the shallow water table, can translate into important reductions on the expected pesticide retention and uncertainty controlled by field conditions (soils, hydraulic loading, pesticide characteristics).

#### 4. Summary and conclusions

In this study, we coupled a new infiltration algorithm under shallow water table conditions (SWINGO, developed in companion paper) with a commonly used event based vegetative filter strips model (VFSMOD). The coupled model takes into account the dynamic interactions among water table, surface runoff, sediment and pesticide filtration in a vegetative filter strip. The model was applied to two different experimental sites with contrasted soils and rainfall conditions. The direct testing of the uncalibrated model under limited experimental conditions showed promising results. Simulations varying the water table depth for two experimental sites provided interesting insights on the effect on VFS efficiencies to reduce overland flow, sediment and pesticides. While the VFS surface flow, sediment and pesticide reduction responses are very sensitive when the water table is close to the surface, the effect is lost after a threshold depth around 1.5 m for the experimental sites condition, consistent with previous field studies (Dosskey et al., 2006, Lacas et al., 2012). For depths larger than the threshold, the model showed physical consistency when compared to a common Green-Ampt solution (with no water table assumptions). More comprehensive global sensitivity and uncertainty analyses (GSA) for the two sites revealed that the effectiveness of the VFS was markedly reduced in the presence of the shallow water table, and in this case the VFS response is more complex, dominated by interactions between surface, subsurface and transport processes. The most important factors controlling the expected variability of water and pesticide reductions are water table depth and saturated hydraulic conductivity of the soil, but their importance also depends on sediment characteristics controlled by the soil type and hydraulic loading of the event. Uncertainty in the pesticide reduction, driven by water or sediment reduction, also depends on the pesticide sorption properties (Koc).

360 This work suffers from some limitations. Firstly, limited field experimental data is available for detailed studies of the response of a VFS under alternative conditions of deep and shallow water table. Further laboratory and field research should address this limitation, where exhaustive experimental datasets must be compiled to reduce the uncertainty in the identification of sensitive input factors controlling the measured and simulated responses studied here. Secondly, although two contrasting case studies were selected, the results presented here are limited to these studies, and further analysis will be needed for other local, regional and larger scales.

365 The combination of the limited experimental, testing, evaluation under contrasting set of conditions, and physical consistency with other models indicate the robustness of the revised model for use in VFS sizing and evaluation of potential losses of efficiency under shallow water table conditions. Since VFS are commonly placed near streams and these areas can



370 suffer seasonal shallow water conditions, this tool fills an important gap in environmental management and analysis. For  
example, in Europe VFS are often prescribed along rivers drainage networks without objective assessment of their efficiency  
375 during winter wet periods (Carluer et al., 2017). In the US, the historical topography-based approach, which links priority for  
buffers to locations where runoff water converges from uplands and saturates the soil, often results in placement on  
bottomlands next to streams (Dosskey and Qiu 2011). Alternative targeted placement of buffers based on soil characteristics  
and conductivity can improve the efficiency of the buffers (Dosskey et al., 2006). However, both placement methods  
380 disregard seasonal shallow water table effects that can now be mechanistically assessed with the improved physical model  
developed herein. For the case of the regulatory assessment of pesticides, currently long-term exposure frameworks in  
Europe and the USA disregard the potential effects that shallow water effects might have in reducing the effectiveness of in-  
label mitigation practices like VFS. Results from this study support the critical need to incorporate in these environmental  
exposure assessments the effects of a shallow water table when present.

#### Author contribution

380 CL and RMC participated in the model coupling, coding the GSA application, analysis and interpretation of the results and  
writing of the manuscript.

#### Acknowledgements

The authors wish to thank Nadia Carluer for the field testing dataset and selection of the study sites, and review of the paper.  
Marilisa Letey helped with the literature review for this manuscript. CL acknowledges TOPPS-PROWADIS for partial  
385 project funding. The second author received support from the UF Research Foundation Professorship, UF Water Institute  
Fellowship, and USDA NIFA Award No: 2016-67019-26855. The authors also thank the University of Florida Research  
Computing (<http://researchcomputing.ufl.edu>) for providing high performance computational resources and support that  
have contributed to the research results reported in this publication.



## 390 References

- Abu-Zreig, M.: Factors Affecting Sediment Trapping in Vegetated Filter Strips: Simulation Study Using VFSMOD, *Hydrol. Proc.*, 15, 1477, doi:10.1002/hyp.220, 2001.
- Adamiade, V: Influence d'un fossé sur les écoulements rapides au sein d'un versant. Université Pierre et Marie Curie, Spécialité Géosciences - Ressources Naturelles, Paris VI., 2004.
- 395 Arora, K., Mickelson, S.K., Helmers, M.J., Baker, J.L.: Review of Pesticide Retention Processes Occurring in Buffer Strips Receiving Agricultural Runoff1. *JAWRA Journal of the American Water Resources Association* 46, 618–647, doi:10.1111/j.1752-1688.2010.00438.x, 2010.
- Asmussen, L.E., White, A.W., Hauser, E.W., Sheridan, J.M.: Reduction of 2,4-D Load in Surface Runoff Down a Grassed Waterway. *J. Environ. Qual.*, 6, 159. doi:10.2134/jeq1977.00472425000600020011x, 1977.
- 400 Balderacchi, M., Perego, A., Lazzari, G., Muñoz-Carpena, R., Acutis, M., Laini, A., Giussani, A., Sanna, M., Kane, D., Trevisan, M. Avoiding social traps in the ecosystem stewardship: The Italian Fontanile lowland spring. *Sci. Total Env.* 539, 526-535, doi:10.1016/j.scitotenv.2015.09.029, 2016.
- Barfield, B. J., E. W. Tollner, and J. C. Hayes: The use of grass filters for sediment control in strip mining drainage. Vol. I: Theoretical studies on artificial media. Pub. No. 35–RRR2–78. Lexington, Ky.: University of Kentucky, Institute for Mining and Minerals Research, 1978.
- 405 Benoit, P., Barriuso, E., Vidon, P., Réal, B.: Isoproturon Sorption and Degradation in a Soil from Grassed Buffer Strip. *J. Environ. Qual.*, doi:10.2134/jeq1999.00472425002800010014x, 28,121, 1998.
- Boivin, A., Lacas, J.G., Carluer, N., Margoum, C., Gril, J.-J., Gouy, V.: Pesticide leaching potential through the soil of a buffer strip in the river Morcille catchment (Beaujolais). XIII Symposium Pesticide Chemistry - Environmental Fate and Human Health, Piacenza, Italie, 2007.
- 410 Bouwer, H.: Infiltration of water into nonuniform soil. *Journal of Irrigation and Drainage Division* 95:451–462, 1969.
- Carluer, N., Lauvernet, C., Noll, D., Muñoz-Carpena, R.: Defining context-specific scenarios to design vegetated buffer zones that limit pesticide transfer via surface runoff, *Sci. Total Environ.*, 575, 701-712, doi:10.1016/j.scitotenv.2016.09.105, 2017.
- 415 Chu, S.T.: Infiltration during unsteady rain. *Water Resour. Res.*, 14, 3, 461-466, doi:197810.1029/WR014i003p00461, 1978.
- Cukier, R.I., Levine, H.B., Shuler, K.E.: Nonlinear sensitivity analysis of multiparameter model systems. *J. Comput. Physics*, 26, 1, 1978.
- Dosskey, M.G.: Toward quantifying water pollution abatement in response to installing buffers on crop land. *Environ Manage* 28, 577–598, doi: 10.1007/s002670010245, 2001.



- 420 Dosskey, M.G., Helmers, M.J., Eisenhauer, D.E.: An Approach for Using Soil Surveys to Guide the Placement of Water Quality Buffers. *Journal of Soil and Water Conservation* 61, 344–354, 2006.
- Dosskey, M.G., M.J. Helmers, D.E. Eisenhauer, T.G. Franti and K.D. Hoagland: Assessment of concentrated flow through riparian buffers. *Journal of Soil and Water Conservation*, 57:336–343, 2002.
- Dukes, M.D., Evans, R.O., Gilliam, J.W., Kunickis, S.H.: Effect of Riparian Buffer Width and Vegetation Type on Shallow  
425 Groundwater Quality in the Middle Coastal Plain of North Carolina, *Trans. of ASABE* 45:327, 2002.
- EU-JRC. 2004. SIMLAB Version 2.2.1. Simulation Environment for Uncertainty and Sensitivity Analysis. Joint Research Centre of the European Commission, Ispra, Italy. <https://ec.europa.eu/jrc/en/samo/simlab> (accessed July 2017)
- Faivre, R., Iooss, B., Mahévas, S., Makowski, D., Monod, H.: *Sensitivity Analysis and Exploration of Models*. Editions Quae, in French, 2013.
- 430 Fontaine, A.: Optimizing the size of grassed buffer strips to limit pesticides transfer from land to surface water in overland flow », Cranfield University, UK, MSc Thesis, 2010.
- Fox, A.L., D.E. Eisenhauer, M.G. Dosskey: Modeling water and sediment trapping by vegetated filters using VFSSMOD: comparing methods for estimating infiltration parameters. *ASAE Paper*, 052118. Joseph, 2005.
- Fox, G., Muñoz-Carpena, R., Sabbagh, G.: Influence of flow concentration on parameter importance and prediction  
435 uncertainty of pesticide trapping by vegetative filter strips. *J. Hydrol.*, 384, 164-173, doi:10.1016/j.jhydrol.2010.01.020, 2010.
- Gatel, L., Lauvernet, C., Carluer, N., and Paniconi, C.: Effect of surface and subsurface heterogeneity on the hydrological response of a grassed buffer zone, *Journal of Hydrology*, 542, 637-647, 10.1016/j.jhydrol.2016.09.038, 2016.
- Haan CT, Barfield BJ, Hayes JC.: *Design hydrology and sedimentology for small catchments*. San Diego, Calif.: Academic  
440 Press, 1994.
- Han, J., Wu, S., Allan, C.: Suspended sediment removal by vegetative filter strip treating highway runoff. *Journal of Environmental Science and Health*, 40:1637–1649, doi:10.1081/ESE-200060683, 2005.
- Johnson, S.R., Burchell, M.R. R.O. Evans, D.L. Osmond, Gilliam, J.W.: Riparian Buffer Located in an Upland Landscape Position Does Not Enhance Nitrate-Nitrogen Removal, *Ecol. Engineering*, 52, 252, doi:10.1016/j.ecoleng.2012.11.006,  
445 2013.
- Khare, Y.P., R. Muñoz-Carpena., R.W. Rooney. and C.J. Martinez: A multi-criteria trajectory-based parameter sampling strategy for the screening method of elementary effects. *Environ. Modell. Softw.* 64,230-239, doi:10.1016/j.envsoft.2014.11.013, 2015.
- Kuo, Y.M. and R. Muñoz-Carpena: Simplified modeling of phosphorus removal by vegetative filter strips to control runoff  
450 pollution from phosphate mining areas, *J. of Hydrol.*, 378, 343-354, doi:10.1016/j.jhydrol.2009.09.039, 2009.



- Lacas, J.-G., 2005. Processus de dissipation des produits phytosanitaires dans les zones tampons enherbées. Etude expérimentale et modélisation en vue de limiter la contamination des eaux de surface. Université Montpellier II. Sciences et techniques du Languedoc.
- Lacas, J.-G., Voltz, M., Gouy, V., Carluier, N., Gril, J.-J.: Using grassed strips to limit pesticide transfer to surface water: a  
455 review. *Agron. Sustain. Dev.* 25, 253–266, doi:10.1051/agro:2005001, 2005.
- Lacas, J.-G., Carluier, N., Voltz, M.: Efficiency of a Grass Buffer Strip for Limiting Diuron Losses from an Uphill Vineyard Towards Surface and Subsurface Waters. *Pedosphere*, 22, 580-592, doi:10.1016/S1002-0160(12)60043-5, 2012.
- Lane, K. S., and Washburn, S. E.: Capillary tests by capillarimeter and by soil filled tubes. *Proc. Highway Research Board*, 26, 460–473, 1946.
- 460 Lighthill, M.J., Whitham, C.B.: On kinematic waves: flood movement in long rivers. *Proc. R. Soc. London Ser. A* , 22, 281-316, 1955.
- Louchart, X., M. Voltz, P. Andrieux, et R. Moussa: Herbicide Transport to Surface Waters at Field and Watershed Scales in a Mediterranean Vineyard Area, *Journal of Environmental Quality*, 30:982, 2001.
- Madrigal-Monarez, I.: Sorption of pesticides in soil from grassed and forested buffer zones: the role of organic matter.  
465 INAPG PhD Thesis (AgroParisTech), 2004.
- Malaj E., P.C. von der Ohe, M. Grote, R. Kühne, C.P. Mondy, P. Usseglio-Polatera, W. Brack, and R.B. Schäfer. Organic chemicals jeopardize the health of freshwater ecosystems on the continental scale. *PNAS* 111, 26, 9549-9554. doi:10.1073/pnas.1321082111, 2014.
- Mein, R.G., Larson, C.L.: Modelling the infiltration component of the rainfall-runoff process, *Bulletin 43*, University of  
470 Minnesota, MN, Water Resources Research Center, 1971.
- Meyer, P.D.; Rockhold, M.L. & Gee, G.W. Uncertainty analyses of infiltration and subsurface flow and transport for SDMP sites, report, September 1, 1997; Washington D.C.. ([digital.library.unt.edu/ark:/67531/metadc690558/](http://digital.library.unt.edu/ark:/67531/metadc690558/): accessed July 7, 2017), University of North Texas Libraries, Digital Library, [digital.library.unt.edu](http://digital.library.unt.edu); crediting UNT Libraries Government Documents Department.
- 475 Muñoz-Carpena, R., C.T. Miller, and J.E. Parsons: A Quadratic Petrov-Galerkin Solution for Kinematic Wave Overland Flow. *Water Resour. Res.* 29, 8, 2615-2627, 1993a.
- Muñoz-Carpena, R., Parsons, J.E., Gilliam, J.W.: Numerical Approach to the Overland Flow Process in Vegetative Filter Strips, *Trans. of ASABE* 36, 3, 761-770, 1993b.
- Muñoz-Carpena, R., Parsons, J.E., Gilliam, J.W.: Modeling hydrology and sediment transport in vegetative filter strips. *J.*  
480 *Hydrol.*, 214, 111–129. doi:10.1016/S0022-1694(98)00272-8, 1999.
- Muñoz-Carpena, R. and Parsons, J. E.: A design procedure for vegetative filter strips using VFSSMOD-W, *Transactions of the ASAE* 47(6), 1933—1941, doi :10.13031/2013.17806, 2004.



- Muñoz-Carpena, R., Z. Zajac, et Y.-M. Kuo: Global sensitivity and uncertainty analyses of the water quality model VFSMOD., *Trans. of ASABE* 50:1719-1732, 2007.
- 485 Muñoz-Carpena, R., Fox, G., Sabbagh, G.: Parameter Importance and Uncertainty in Predicting Runoff Pesticide Reduction with Filter Strips. *Journal of Environmental Quality*, 39,630, doi:10.2134/jeq2009.0300, 2010.
- Muñoz-Carpena, R. A. Ritter, G.A. Fox and O. Perez-Ovilla: Does mechanistic modeling of filter strip pesticide mass balance and degradation affect environmental exposure assessments? *Chemosphere* 139:410-421. doi:10.1016/j.chemosphere.2015.07.010, 2015.
- 490 Ohliger, R., Schulz, R.: Water body and riparian buffer strip characteristics in a vineyard area to support aquatic pesticide exposure assessment, *Sci. Total Environ.*, 408, 5405-5413, doi:scitotenv.2010.08.025, 2010.
- Pan, D.; Gao, X.; Dyck, M.; Song, Y.; Wu, P., Zhao, X.: Dynamics of runoff and sediment trapping performance of vegetative filter strips: Run-on experiments and modeling *Science of The Total Environment*, 593–594, 54-64, 2017.
- Parlange, J.-Y., Haverkamp, R., Starr, J. L., Fuentes, C., Malik, R. S., Kumar, S., and Malik, R. K.: Maximal capillary rise flux as a function of height from the water table. *Soil Sci.*, 150, 6, 896–898, 1990.
- 495 Patty, L., Réal, B., Gril, J.J.: The use of grassed buffer strips to remove pesticides, nitrate and soluble phosphorus compounds from runoff water. *Pesticide science*, 243:251, 1997.
- Perez-Ovilla, O.: Modeling runoff pollutant dynamics through vegetative filter strips: a flexible numerical approach. Ph.D. Thesis, University of Florida, Gainesville, 195pp, 2010.
- 500 Poletika, N.N., Coody, P.N., Fox, G.A., Sabbagh, G.J., Dolder, S.C., White, J.: Chlorpyrifos and Atrazine Removal from Runoff by Vegetated Filter Strips: Experiments and Predictive Modeling. *J. Environ. Qual.*, 38, 1042–1052. doi:10.2134/jeq2008.0404, 2009.
- Rawls WJ, Brakensiek DL, Miller N.: Green-Ampt infiltration parameters from soils data. *J. Hydraul. Eng.*, 109(1), 62-70, 1983.
- 505 Reichenberger S, Bach M, Skitschak A, Frede H-G.: Mitigation strategies to reduce pesticide inputs into ground- and surface water and their effectiveness: a review. *Sci. Total Environ.*, 384, 1-35, doi:10.1016/j.scitotenv.2007.04.046, 2007.
- Roberts, W.M., M.I. Stutter, and P.M. Haygarth: Phosphorus Retention and Remobilization in Vegetated Buffer Strips: A Review. *J. Environ. Qual.* 41:389–399 (2012) doi:10.2134/jeq2010.0543, 2012.
- Rohde, W.A., L.E. Asmussen, E.W. Hauser, R.D. Wauchope: Trifluralin movement in runoff from a small agricultural watershed. *J. Environ. Qual.*, 9, pp. 37–42, 1980.
- 510 Sabbagh, G.J., Fox, G.A., Kamanzi, A., Roepke, B., Tang, J.-Z.: Effectiveness of Vegetative Filter Strips in Reducing Pesticide Loading: Quantifying Pesticide Trapping Efficiency. *J. Environ. Qual.* 38, 762. doi:10.2134/jeq2008.0266, 2009.
- Saltelli A., S. Tarantola, F. Campolongo, M. Ratto: *Sensitivity Analysis in Practice: A Guide to Assessing Scientific Models*. John Wiley & Sons, Chichester, 2004.



- 515 Saltelli, A., Annoni, P., Azzini, I., Campolongo, F., Ratto M., Tarantola, S.: Variance Based Sensitivity Analysis of Model Output. Design and Estimator for the Total Sensitivity Index. *Computer Physics Communications* 181:259, 2010.
- Saltelli, A., Ratto, M., Andres, T., Campolongo, F., Cariboni, J., Gatelli, D., Saisana, M., Tarantola, S.: *Global Sensitivity Analysis: The Primer*. John Wiley & Sons, Chichester, 2008.
- Saltelli, A., Tarantola, S., Chan, K.P.-S.: A Quantitative Model-Independent Method for Global Sensitivity Analysis of  
520 Model Output, *Technometrics* 41:39, 1999.
- Simpkins, W., Wineland, T., Andress, R., Johnston, D., Caron, G., Isenhardt, T., Schultz, R. : Hydrogeological constraints on riparian buffers for reduction of diffuse pollution: examples from the Bear Creek watershed in Iowa, USA, *Water Science and Tech.* 45, 9, 2002.
- Skaggs, R.W., Khaheel, R., 1982. Infiltration, Ch. 4, In: *Hydrologic modeling of small watersheds*. C.T. Haan, H.P. Johnson,  
525 D.L. Brakensiek, Eds., St. Joseph, MI, ASAE. pp. 121–168.
- Souillier, C., Y. Coquet, V. Pot, P. Benoit, B. Réal, C. Margoum, B. Laillet, C. Labat, P. Vachier, A. Dutertre: Capacités de stockage et d'épuration des sols de dispositifs enherbés vis-à-vis des produits phytosanitaires. Première partie : Dissipation des produits phytosanitaires à travers un dispositif enherbé ; mise en évidence des processus mis en jeu par simulation de ruissellement et infiltrométrie. *Etude et Gestion des Sols*, 9,269, 2002.
- 530 Stehle, S., and R. Schulz: Agricultural insecticides threaten surface waters at the global scale. *PNAS* 112, 18, 5750-5755, doi:10.1073/pnas.1500232112, 2015.
- Syversen, N. and M. Bechmann: Vegetative buffer zones as pesticide filters for simulated surface runoff. *Ecological Engineering* 22:175–184, 2004.
- Tarantola, S., N. Giglioli, J. Jesinghaus, et A. Saltelli: Can Global Sensitivity Analysis Steer the Implementation of Models  
535 for Environmental Assessments and Decision-Making? *Stochastic Environmental Research and Risk Assessment*, 16, 63, 2002.
- Terzaghi, K.: *Theoretical soil mechanics*, Wiley, New York, 1943.
- Tollner, E.W., Barfield, B.J, Haan, C.T., Kao, T.Y.: Suspended sediment filtration capacity of simulated vegetation. *Trans. ASAE* 19, 4, 678-682, 1976.
- 540 Tomer, M.D., M.G. Dosskey, M.R. Burkart, D.E. James, M.J. Helmers and D.E. Eisenhauer: Methods to prioritize placement of riparian buffers for improved water quality. *Agroforestry Systems* 75, 1, 17-25, 2009.
- UIPAC: The PPDB Pesticide Properties Database. International Union of Pure and Applied Chemistry (UIPAC), Research Triangle Park, NC (USA) <http://sitem.herts.ac.uk/aeru/iupac/>, 2007.
- Winchell, M.F., Jones, R.L., Estes, T.L.: Comparison of models for estimating the removal of pesticides by vegetated filter  
545 strips. *ACS Symp. Ser.* 273-286, 2011.
- Woolhiser, D.A., R.E. Smith, et D.C. Goodrich: *KINEROS, A kinematic runoff and erosion model: documentation and user manual*, 1990.



Yang, J.: Convergence and uncertainty analyses in Monte-Carlo based sensitivity analysis. *Environ. Modell. Softw.* 26:444, 2011.

550 Yu, C., R. Muñoz-Carpena, B. Gao and O. Perez-Ovilla: Effects of ionic strength, particle size, flow rate, and vegetation type on colloid transport through a dense vegetation saturated soil system: Experiments and modeling. *J. of Hydrology*, 499, 316-323, doi:10.1016/j.jhydrol.2013.07.004, 2013.

White, M. J. and Arnold, J. G.: Development of a simplistic vegetative filter strip model for sediment and nutrient retention at the field scale, *Hydrol. Proc.*, 23, 11, doi:10.1002/hyp.7291, 2009.



555 **Table 1. Characteristics of the field studies utilized for sensitivity–uncertainty analyses of shallow water table effects on VFS performance**

Study	Authors	Lacas (2005); Lacas et	Madrigal-Monarez
		al. (2012)	(2004), Adamiade (2004)
Location, climate		Morcille, Mediterranean semi-continental	Jaillère, Temperate oceanic
Event description	Rainfall (mm)	15	10.7
	Rainfall duration (hr)	2.1	3
	Inflow volume (mm)	0.847	6.347
	Inflow duration (hr)	2.1	7.9
	Hydraulic loading (rainfall + incoming runoff) (m <sup>3</sup> )	2.48	25.9
	Shallow water table depth (m)	2.5 (0.4-2.5)	0.8 (0.4-2)
	Source field area (m <sup>2</sup> )	2500	4000
Soil description	Soil name	Cambisol-luvisol	Stagnic-luvisol
	USDA texture	Sandy-loam	Silty-clay
VFS description	Length (direction of flow)×width	6 x 4m	5 x 10m
	slope	28%	4%
	Field-to-filter area ratio	110	100
	Vegetation	Ray-grass (20 years)	Ray-grass (7 years)
Pesticides (K <sub>oc</sub> , ml/g)		Isoproturon (144)	Isoproturon (144)
		Tebuconazole (769)	Diflufenican (3000)



558 Table 2. Input factors base values and selected statistical distributions at the case study sites.

Input factor (units)	Description	Morcille		Jaillière	
		Base value	Distribution	Base value	Distribution
<b>Hydrological inputs</b>					
FWIDTH (m)	Effective flow width of the strip	4.0	$U(4.0, 4.4)$	10.0	$U(9.0, 10.0)$
VL (m)	Length in the direction of the flow	6.0	$U(5.4, 6.0)$	5.0	$U(5.0, 5.5)$
RNA ( $s\ m^{-1/3}$ )	Filter Manning's roughness $n$ for each segment	0.2	$T(0.1, 0.2, 0.3)$	0.2	$T(0.1, 0.2, 0.3)$
SOA (-)	Filter slope for each segment	0.25	$U(0.20, 0.30)$	0.03	$U(0.02, 0.04)$
VKS ( $m\ s^{-1}$ )	Soil vertical saturated hydraulic conductivity in the VFS	4.58E-5	$LN(-10.6676, 0.69)$	2.50E-6	$LN(13.0, 0.69)$
SAV (m)	Green-Ampt's average suction at wetting front	0.110	$U(0.088, 0.132)$	0.1668	$U(0.13, 0.20)$
OI (-)	Initial soil water content, $\theta_i$	0.22	$U(0.1, 0.35)$	0.15	$U(0.12, 0.18)$
OS (-)	Saturated soil water content, $\theta_s$	0.4	$N(0.4, 0.03)$	0.4	$N(0.4, 0.03)$
SCHK (-)	Relative distance from the upper filter edge where check for ponding conditions is made (i.e., 1 = end; 0 = beginning)	0.5	$U(0, 1)$	0.5	$U(0, 1)$
L (m) <sup>†</sup>	Shallow water table depth from soil surface	1.0	$U(0.4, 2.5)$	0.8	$U(0.4, 2)$
OR (-) <sup>†</sup>	Residual soil water content, $\theta_r$	0.038	$N(0.038, 0.03)$	0.07	$N(0.07, 0.03)$
VGALPHA ( $m^{-1}$ ) <sup>†</sup>	van Genuchten soil characteristic curve parameter ( $\alpha$ )	10.0	$N(10, 2)$	1.18	$N(1.18, 0.05)$
VGN (-) <sup>†</sup>	van Genuchten soil characteristic curve parameter ( $n$ ), $m=1-1/n$	1.52	$N(1.52, 0.05)$	1.45	$N(1.45, 0.05)$
<b>Vegetation inputs</b>					
SS (cm)	Average spacing of grass stems	1.6	$U(1.3, 2.1)$	1.6	$U(1.3, 2.1)$
VN ( $s\ cm^{-1/3}$ )	Filter media (grass) modified Manning's $n_m$ (cylindrical = 0.012)	0.012	$T(0.0084, 0.012, 0.016)$	0.012	$T(0.0084, 0.012, 0.016)$
H (cm)	Filter grass height	15.0	$U(10, 35)$	15.0	$U(10, 35)$



<b>Sedimentation inputs</b>	
VN2 ( $s\ m^{-1/3}$ )	Bare surface Manning's n for sediment inundated area in VFS 0.013 T(0.011,0.013,0.04) 0.02 T(0.011,0.02,0.04)
DP (cm)	Sediment particle size diameter (d50) 0.0099 U(3.80E-3,1.60E-2) 0.0029 U(2.00E-4,3.69E-3)
COARSE (-)	Fraction of incoming sediment with particle diameter > 0.0037 cm (coarse fraction routed through wedge as bed load) [unit fraction, i.e. 100% = 1.0] 0.55 U(0.51,0.6) 0.45 U(0.4,0.49)
<b>Pesticide inputs</b>	
KOC (ml/g)	Organic carbon sorption coefficient for simulated pesticide
Isoproturon	144 T(36,144,241) 144 T(36,144,241)
Tebuconazole	769 T(102,769,1249) -
Diflufenican	- 3000 T(1622,3000,7431)
PCTOC (%)	Percentage of organic carbon in the soil 1.2 U(1.18,2.5) 3.78 U(1.4,7)
PCTC (%)	Percentage clay in the soil 12 U(11,15) 22 U(19.8,25.5)

559 † Parameters of the new infiltration under shallow water table component (SWINGO); ‡Statistics of the assigned distributions, uniform: U(mix,max), triangular:

560 T(min,mean,max), log-normal: LN( $\mu_y, \sigma_y$ ), normal: N( $\mu_s, \sigma_s$ ). LN and N distributions are truncated between (0,001,0.999).

561 **Figure captions**

562 **Figure 1:** Conceptual model of VFSSMOD showing the coupling between overland flow, soil infiltration and  
563 redistribution, sediment and pesticide components. Solid lines indicate required processes and their interactions, and  
564 dashed lines are optional, user selected components. The selection of infiltration under either a) deep water table  
565 (extended Green-Ampt, GAMPT), or b) shallow water table (SWINGO) is highlighted.

566 **Figure 2:** Details of the dynamic coupling of (a) the overland flow and sediment and pesticide transport through the  
567 VFS (contained in VFSSMOD), with (b) the new infiltration and soil water redistribution with shallow water  
568 component (SWINGO). Colors indicate water (blue), sediment (brown) and pesticide (red) components.  $V$ ,  $M$  and  $m$   
569 indicate water, sediment and pesticide mass moving through the filter, where subscripts indicate incoming ( $i$ ),  
570 outgoing ( $o$ ), in sediment ( $sed$ ), on the filter ( $f$ ), infiltrated ( $F$ ), in mixing-layer ( $ml$ ) and in runoff ( $ro$ ). Other symbols  
571 are defined in the text.

572 **Figure 3:** Location of experimental VFS sites: Jaillièrre, North-West of France, maize crops on a flat silty-clay soil  
573 under Temperate oceanic climate; Morcille, South-East of France, vineyards on a sandy-loam soil under  
574 Mediterranean semi-continental climate. Morcille is located at  $46^{\circ}10'31.3''N$  -  $4^{\circ}38'11.2''E$  and Jaillièrre at  
575  $47^{\circ}27'6.25''N$  -  $0^{\circ}57'58.37''O$ , in GPS coordinates.

576 **Figure 4:** Hydrological response of the VFS at the study sites. (a) Event at Morcille Aug. 17, 2004 with  $L=2.5$  m,  
577 showing comparison of measured outflow (symbols) and VFSSMOD simulations (lines). The dashed  $Q_{out}$  line for  
578  $L=2.5$  m corresponds to average conditions for that event ( $K_s = 4.58E-05$  m/s), and the grey envelope represents  
579 outflow variability due to uncertainty of measured hydraulic conductivity. (b) Event at Jaillièrre on February 16, 1997  
580 with  $L=0.8$  m, without outflow measurements.  $Q_{in}$  and  $Q_{out}$  represent surface inflow and outflow at the VFS. The  
581 potential effect on overland outflow of alternative water table depths in those events is represented by the dotted lines  
582 for  $L=0.4$  (a) and  $2.0$  m (b).

583 **Figure 5:** Change in  $dQ$  (reduction of surface water),  $dE$  (reduction of sediment) and  $dP$  (reduction of pesticide  
584 Isoproturon) with water table depth for experimental events in Fig. 4a-b. Grey area indicates water table depths  
585 where influence over surface outputs on the VFS is no longer observed.

586 **Figure 6:** Morris elementary effects results for  $dQ$  (reduction of surface water),  $dE$  (reduction of sediment) and  $dP$   
587 (reduction of pesticide Isoproturon) on Jaillièrre (a-f) and Morcille (g-l) sites, without water table (no WT) and with  
588 water table (WT) present.

589 **Figure 7:** Global sensitivity analysis eFAST results for  $dQ$  (reduction of surface water),  $dE$  (reduction of sediment)  
590 and  $dP$  (reduction of pesticide Isoproturon) outputs on the Jaillièrre (a-f) and Morcille (g-l) sites, without water table  
591 (no WT) and with water table (WT). Grey and black bars represent first order ( $S_i$ ) total sensitivity ( $S_{Ti}$ ) indices

592 **Figure 8:** Uncertainty analysis results obtained from eFAST simulations on output variables  $dQ$  (reduction of surface  
593 water),  $dE$  (reduction of sediment),  $dP$  (reduction of pesticides) on the Jaillièrre site (a-b) and Morcille (c-d) sites,  
594 without water table (no WT) and with water table (WT). Pesticides are Isoproturon (Iso), Diflufenican (Dif),  
595 Tebuconazole (Teb).

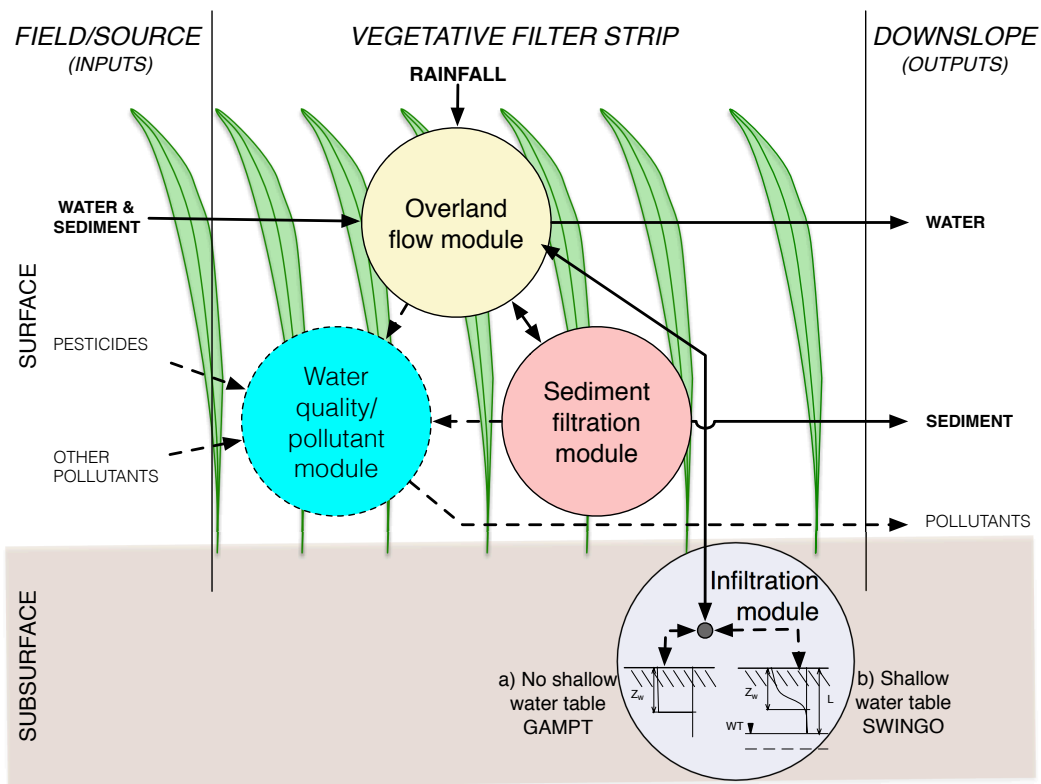


FIG. 1



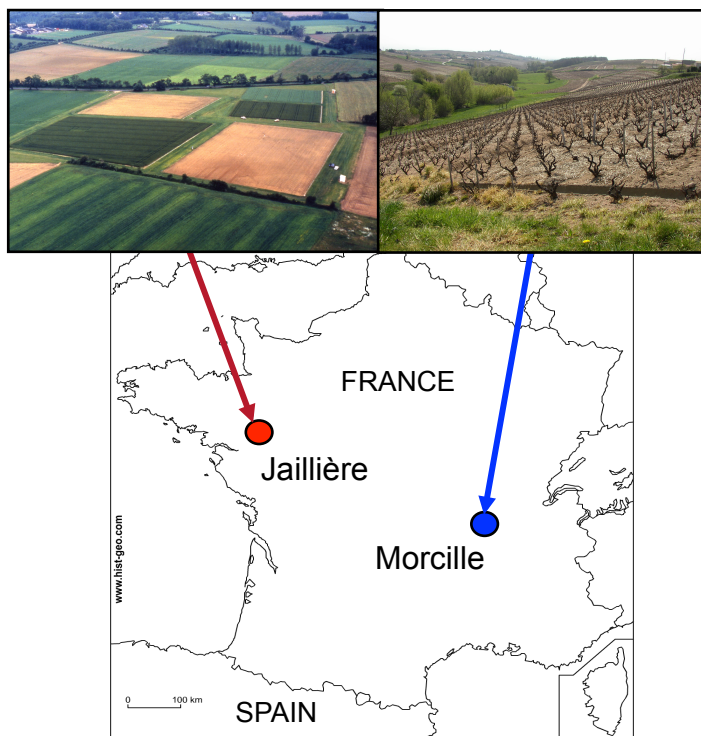


FIG. 3

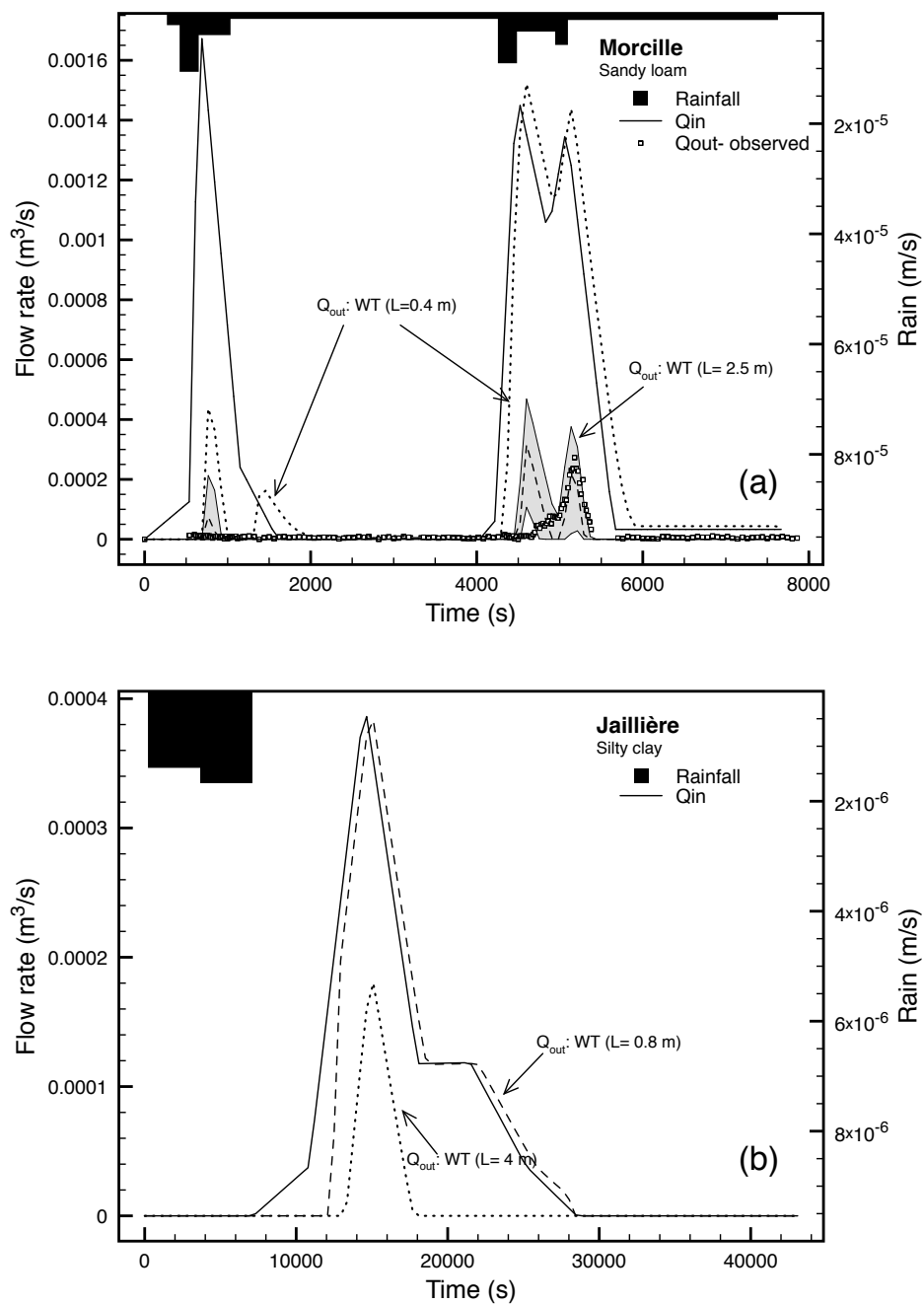


FIG. 4

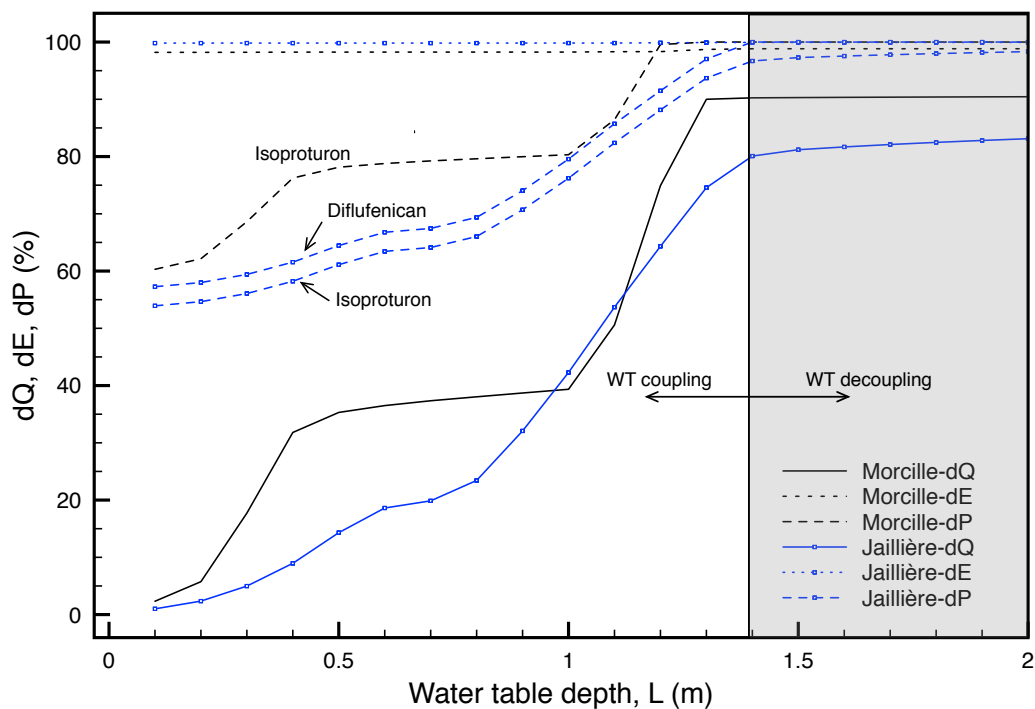


FIG. 5

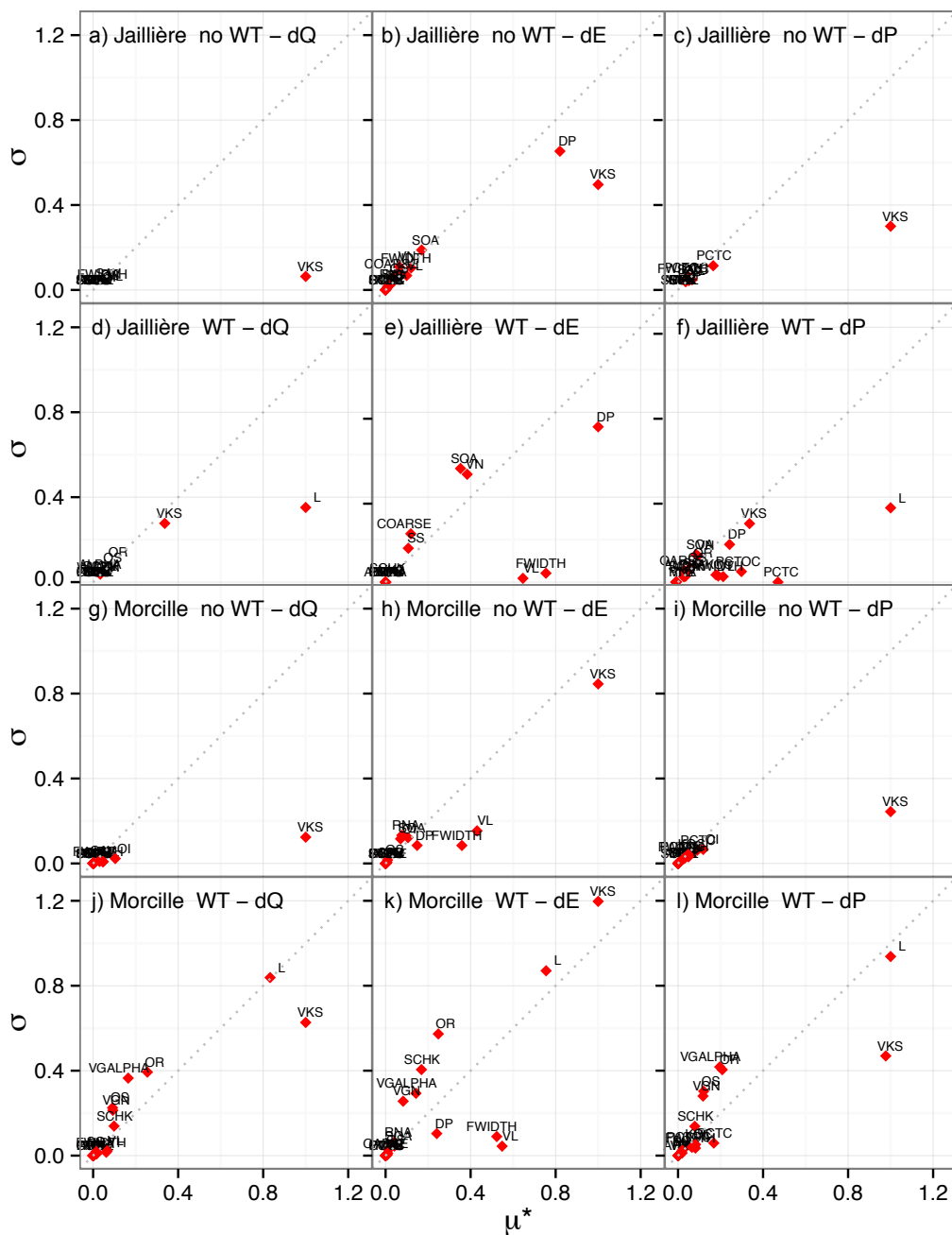


FIG. 6



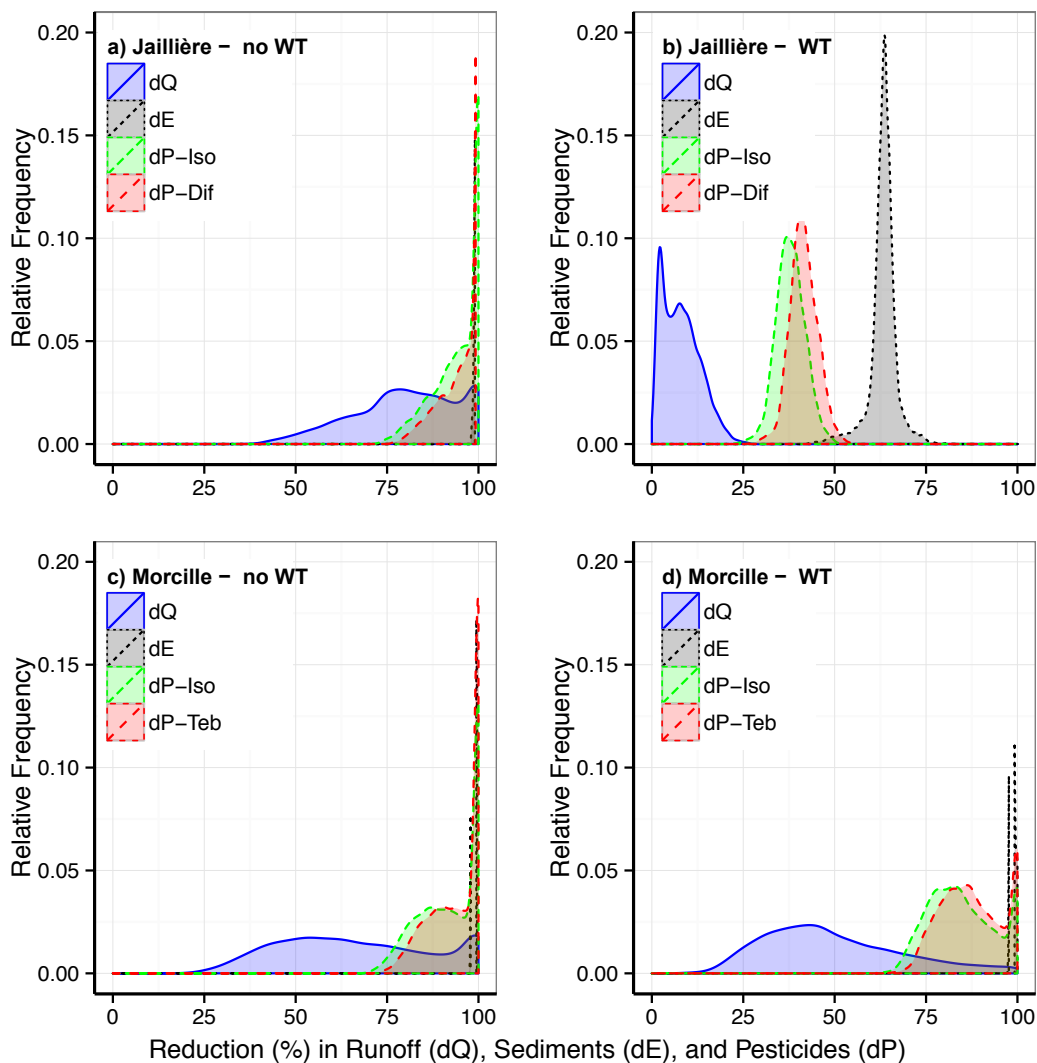


FIG. 8